

Microstructural, Impedance and Conductivity Studies of Vanadium Substituted $\text{Li}_4\text{Ti}_5\text{O}_{12}$ Anode Materials for Li-ion Batteries through Ceramic Method

B. Vikram Babu¹, M. Sushma Reddi², B. Venkateswara Rao³, G. Chandana⁴, A. Rama Krishna⁵, M. V.K.Mehar⁶, L. Usha Kumari⁷, K. Samatha⁸, V. Veeraiah⁹

^{1,4,7,8,9}Department of Physics, Andhra University, Visakhapatnam, India -530003

²Department of Physics, Dr. B. R. Ambedkar University, Srikakulam, 532410, India

³Department of Physics, SS&N College, Narasaraopeta, Guntur, AP State, India

⁵Department of ECE, Aditya College of Engineering and Technology, Kakinada, 533005, India

⁶Department of Physics, PR Govt College, Kakinada, 533001, India

Article Info

Volume 83

Page Number: 9175 - 9180

Publication Issue:

March - April 2020

Article History

Article Received: 24 July 2019

Revised: 12 September 2019

Accepted: 15 February 2020

Publication: 09 April 2020

Abstract

This paper reports the effect of Vanadium (V) substitution in Titanium (Ti) site of spinel lithium titanate ($\text{Li}_4\text{Ti}_5\text{O}_{12}$, LTO) negative electrode materials for Li-ion batteries (LIBs) is studied and analysed. A series of anode materials based on the $\text{Li}_4\text{Ti}_{5-x}\text{V}_x\text{O}_{12}$ ($x=0, 0.0125$ and 0.025) are prepared by simple ceramic route at 900°C for 16 hrs. Their phase formation processes, crystal structures, morphology, cation distribution and electrical properties were studied using XRD, SEM, FTIR and LCR characterization techniques. The X-ray diffraction (XRD) studies confirmed the structure of the materials belonged to cubic spinel group with $Fd-3m$ space group. The topography and morphological structures of phase and distribution of the size of the grains are found to be in the range of 1 to $4\ \mu\text{m}$ as obtained from SEM analysis. FTIR studies also confirmed that the spinel structure in fingerprint region was unchanged when the structure was vanadium doped by 0.025. The impedance of $\text{Li}_4\text{Ti}_{5-x}\text{V}_x\text{O}_{12}$ materials were studied in the frequency ranging from 50 Hz to 1MHz and also in the 30°C - 120°C range of temperature by employing complex impedance spectroscopy (CIS) method. However, both $\text{V}_{0.0125}\text{LTO}$ and $\text{V}_{0.25}\text{LTO}$ doped materials seem to possess good electronic conductivity compared to pure $\text{Li}_4\text{Ti}_5\text{O}_{12}$.

Keywords: Anode Material, Ceramic Route, XRD, SEM, LCR.

INTRODUCTION

Energy and energy sources are much more in need, especially in this modern society. Scarcity of fossil fuels, increasing demand for energy globally and insistence from ecologists to reduce CO_2 emissions has multiplied the demand for unconventional and other substitute energy sources such as nuclear energy, wind energy, solar cells, tidal power, fuel cells and batteries. Among such energy sources, LIBs have been of utmost importance to the advancement of electronics. The Li-ion batteries have become the dominant power sources for

domestic and commercial electronic devices due to their high energy density and low discharge capacity [1-3].

Cubic spinel structured LTO ($\text{Li}_4\text{Ti}_5\text{O}_{12}$) is a novel negative material for advanced LIBs. Spinel LTO material has a lot of merits when compared to presently utilized materials made of graphite. As structural or volume change is not observed during lithium insertion process the LTO can be considered as a material with zero strain [4]. It delivers a constant operating voltage of $\sim 1.5\ \text{V}$ and which is above the decomposition voltage of electrolyte

solvents, but is not high enough to form a solid electrolyte interface (SEI) form. The main disadvantage of the LTO is the low electrical conductivity ($\sigma_e=10^{-13}$ S/cm), which tends to reduce the capacity and rate performance [4-7]. Therefore, improvement in conductivity is required for LTO to be used as negative material in LIB. Many preparation techniques have been suggested to solve the electronic conductivity problem substituting with polyvalent metal ions, namely Ti, Mn, Al, Mg, Nb, Zr, V, Na, Zn, La, Mo and including higher conductivity materials like graphene, carbon and carbon nanotubes to the LTO. Vanadium is chosen for doping as it does not change the lattice constants and the phase of the LTO [8]. The samples were prepared under solid-state synthesis method are its simplicity in synthesis procedure, using low-cost and widely available oxides as the starting materials, suitability for mass-production of cost-efficient powders and environmental friendly technique, which means no toxic or unwanted waste is produced after the synthesis procedure is completed

EXPERIMENTAL TECHNIQUES

The samples were prepared under conventional standard ceramic method. After follows the stoichiometric the raw materials were measured ratios of Li_2CO_3 (Sigma Aldrich, 99.9%), TiO_2 (Sigma Aldrich, 99.9%), V_2O_5 (Merck, 99.9%). This preparation method involves two step procedure. Initially, the raw elements are mixed thoroughly and well ground with agate mortar for 8 hours then the mixture powder is calcinated at a constant temperature of 850°C for 16 hours to completely remove the moisture from the materials so as to free them from gases and impurities. Then calcinated powder is again ground for two hours with adding polyvinyl alcohol (PVA) as an adhesive binder. Then powder materials are pressed with pressure of 7 tons /5 minutes to form pellets of the shape of circular discs. At 900°C temperature, these pellets are sintered for 16 hours in air at $5^\circ\text{C}/\text{minute}$ heating and cooling rate. After polishing the top surfaces of

these pellets, acetone is used to wash them. To make the opposite faces of the sintered pellets act as electrodes silver paste is coated on them. Pellets with size in about 10-12 mm diameter and thickness 1.12 mm are used to study and analyze the electrical properties.

RESULTS AND DISCUSSION

XRD Studies

The XRD characterization were carried out using X-ray Diffractionmeter (PANalytical X-pert pro) for $\text{Li}_4\text{Ti}_{5-x}\text{V}_x\text{O}_{12}$ ($x=0, 0.0125$ and 0.025) samples. The results of the obtained lattice constants can be shown in Table 1 which are good agreement with the other researchers [9-12]. The value of their corresponding Bragg angles and the lattice constants are calculated using Unit Cell software (1997) deduced through least squares refinement of these XRD patterns.

The lattice parameter (a) of compositional material were increases with increasing composition 'x'. This is due to fact that the smaller ionic radii of V ions such as 0.54 for V^{5+} and 0.58 \AA for V^{4+} respectively, while 0.605 for Ti^{4+} and 0.67 \AA for Ti^{3+} respectively and the valence transition from Ti^{4+} to Ti^{3+} by charge compensation is confirmed by XPS studied by some authors [13]. This is expected, as the radius of the V^{5+} (0.54 \AA) is smaller than that of the radius of Ti^{4+} (0.605 \AA) and because of this reason, the lattice constant values have increased. It can be shown in Figure 1 presents the XRD patterns of $\text{Li}_4\text{Ti}_{5-x}\text{V}_x\text{O}_{12}$ ($x=0, 0.0125$ and 0.025) samples. From these figure it can be observed that all the diffraction peaks of doped materials were similar to that of LTO and well defined with sharp and narrow peaks which indicates the high crystallinity of the material. From the figures it can be observed that no impurity peaks were present in the XRD pattern which shows that the compounds are in single phase. Moreover, all the diffraction patterns are in accordance with an ordered spinel structure indexed to the Fd-3m space group symmetry (according to

JCPDS Card No. 49-0207) [14,15]. This specifies that the partial substitution of vanadium for Ti does not alter the structure of LTO. From the Table1 the cell Volumes are calculated for different composition 'x' which are calculated by using the Debye-Scherrer's principle, the crystallite sizes of the synthesized compounds are also calculated. The cell volumes are increases with composition 'x' expect x=0.0125 where decreases due to porosity.

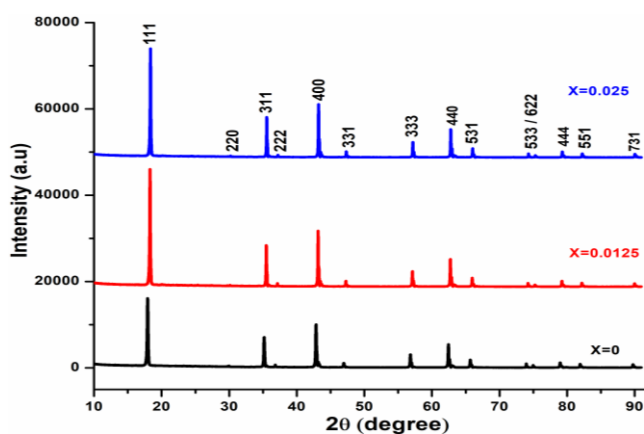


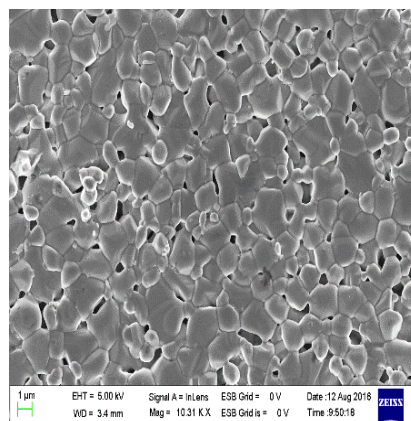
Figure1: XRD patterns for $\text{Li}_4\text{Ti}_{5-x}\text{V}_x\text{O}_{12}$ samples.

Composition	Lattice Parameter a (Å)	Cell Volume $V(\text{Å}^3)$	Grain Size (μm)
x=0	8.3523	582.66	1
x=0.0125	8.3701	580.3972	3.8
x=0.025	8.3902	590.6319	4

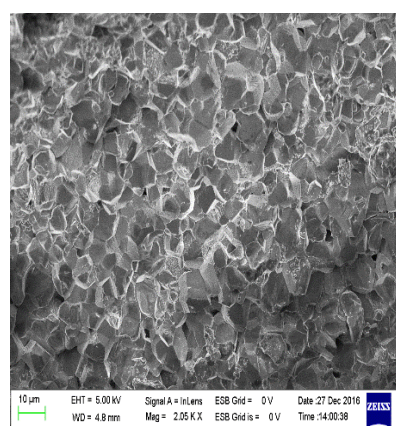
Table 1: Lattice parameters, Cell volumes and Grain sizes of prepared $\text{Li}_4\text{Ti}_5-x\text{V}_x\text{O}_{12}$ (x=0, 0.0125 and 0.025) compounds.

SEM Analysis

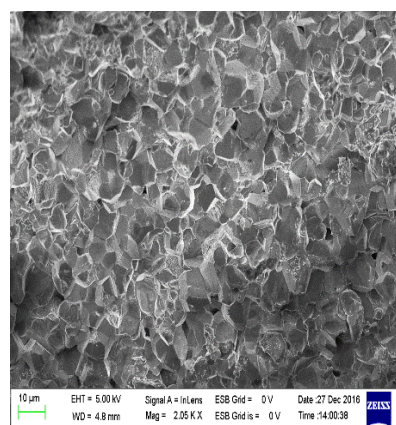
The morphological characterization were carried out using Scanning electron Microscope SEM (CARLZEISS, EVO MA 15) and calculated the grain size using ImageJ software. The grain size increases with increasing composition 'x'. Average measured grain sizes are in the range of 1 μm (for LTO) to 4 μm (for X=0.0125 and 0.25) for doped samples shown in Table 1.



2a) x=0



2b) x=0.0125



2c) x=0.025

Figure 2 (a)-2(c): SEM Micrographs for $\text{Li}_4\text{Ti}_5-x\text{V}_x\text{O}_{12}$ (x=0, 0.0125 and 0.025).

Morphological changes are evidently observed because of the compositional variation of Vanadium doped into the samples. It is also detected that when the dopant composition V increases in the samples, the grain sizes also increase, which is

consistent with the XRD results [16,17]. Moreover, the prepared samples exhibit porous structure, which allows faster penetration of the electrolyte through the anode materials. However some unusually large grains are observed in addition to the smaller grains. Further, as shown in the Figures 2(a) to 2(c), the powder samples display fairly identical grain size distribution, indicating good crystallinity as confirmed by XRD pattern.

FT-IR Analysis:

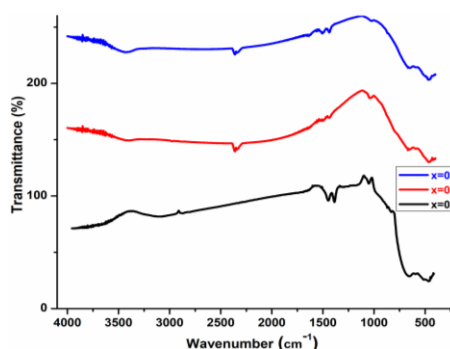


Figure 3: FTIR spectra for $\text{Li}_4\text{Ti}_{5-x}\text{V}_x\text{O}_{12}$ ($x=0$, 0.0125 and 0.025)

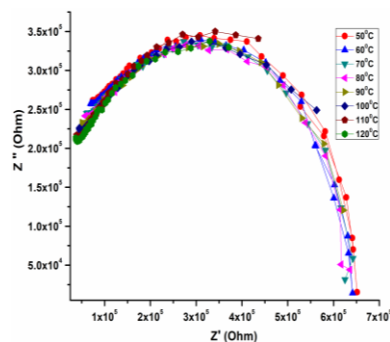
Table 2: FTIR band assignments in $\text{Li}_4\text{Ti}_{5-x}\text{V}_x\text{O}_{12}$ ($x=0$, 0.0125 and 0.025).

Composition	Infrared wavenumber (cm^{-1})			
$x=0$	460	573.1	670	1055
$x=0.0125$	460	573.3	670.2	1053
$x=0.025$	460.7	574	671	1038
Assignment	Li-O)	(Ti-O)	(Ti-O)	(V-O)

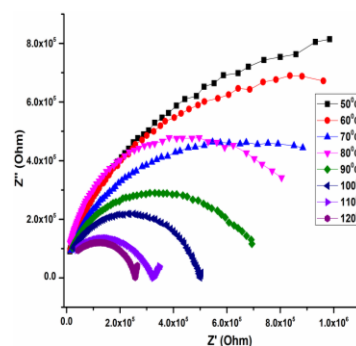
The IR spectra of $\text{Li}_4\text{Ti}_{5-x}\text{V}_x\text{O}_{12}$ ($x=0$, 0.0125 and 0.025) prepared materials are shown in figure 3. Alternating trigonally distorted MO_6 bonds with tetrahedral and octahedral sharing boundaries are present in the cubic spinel framework of $\text{Li}_4\text{Ti}_{5-x}\text{V}_x\text{O}_{12}$ compositions. The Wyckoff positions of $\text{Li}_4\text{Ti}_{5-x}\text{V}_x\text{O}_{12}$ series compounds of 8a and 16c consist of transition metal ions (i.e., Ti and V) and Li-ions correspondingly. The tetrahedral and octahedral sites where there is asymmetric stretching of modes of Li-O and Ti-O bonds in MO_6 lead to the bands observed at about 460.7 cm^{-1} [13,14,17,18]. The identification of the major peaks in these spectra is summarized in Table 2.

Impedance Analysis and Conductivity Study

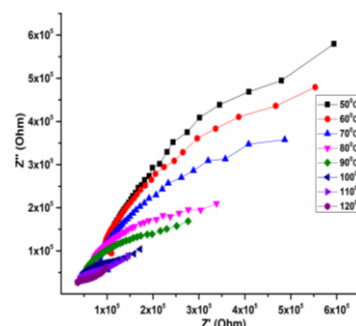
The electrical properties were also studied and the sample are usually obtained from the capacitive and resistive behaviours attributed to the bulk grains, grain boundaries and the defects present at the specimen electrode interface. Figures 4(a)-4(c) shows the Nyquist or Cole-Cole (Z' vs Z'')



a) $x=0$



b) $x=0.0125$



c) $x=0.025$

Figure 4(a)-4(c): Nyquistplots for $\text{Li}_4\text{Ti}_{5-x}\text{V}_x\text{O}_{12}$ ($x=0$, 0.0125 and 0.025)

plots for $\text{Li}_4\text{Ti}_{5-x}\text{V}_x\text{O}_{12}$ ($x=0$, 0.0125 and 0.025) at different temperatures over the frequency range 50 Hz to 1MHz. This evidently shows a decrease in

the diameter of the arcs leading to a rise in electrical conduction as a result of a fall in the resistance of the samples. No other curves are seen in the region of low frequency. Hence, the semicircles of each sample related to intra grain (bulk), grain boundaries and specimen electrode interfaces have to be detached as each one of them have their own exclusive relaxation times. The diameter of the circle is observed to decrease with increase in temperature which may be due to the relaxation process during the conduction of ions. When the concentration of the dopant is made to rise, the arc of the semi curves are decreasing compared to the LTO. It can be seen that the depressed semicircles are shifted to higher frequency region with increase in temperature. The depression of semicircles indicates the non-Debye nature of the material, which is a common property for fast ionic conductors. The merging of Z' versus Z'' at high frequency and temperature may be due to the interfacial charge effect reduction. At high frequencies, contribution of impedance from the grain predominates over the grain boundary [13-15].

At room temperature the observed conductivity values are 1.37×10^{-6} , 6.51×10^{-5} , 3.51×10^{-5} S/cm for $\text{Li}_4\text{Ti}_{5-x}\text{V}_x\text{O}_{12}$ ($x=0, 0.0125$ and 0.025) compounds respectively. It can be found that $\text{Li}_4\text{Ti}_{4.975}\text{V}_{0.025}\text{O}_{12}$ has the highest electrical conductivity 3.51×10^{-5} S/cm.

CONCLUSIONS

The spinel $\text{Li}_4\text{Ti}_{5-x}\text{V}_x\text{O}_{12}$ ($x=0, 0.0125$ and 0.025) anode materials are synthesized by ceramic route and studied the structural, morphological, vibrational and impedance properties systematically. The XRD studies confirms the cubic spinel structure of the FCC structure with a space group of $Fd-3m$. SEM analysis reveals that all the samples exhibit uniform morphology with sphere like particles. This kind of morphology is more significant to achieve high capacity. The vibrational groups are present in $\text{Li}_4\text{Ti}_{5-x}\text{V}_x\text{O}_{12}$ materials as identified from FTIR studies. The electrical

conductivity of $\text{Li}_4\text{Ti}_{5-x}\text{V}_x\text{O}_{12}$ ($x=0, 0.0125$ and 0.025) is higher than the pure $\text{Li}_4\text{Ti}_5\text{O}_{12}$. The impedance study reveals excellent conductivity and was found as 3.51×10^{-5} S/cm at ambient temperature for $x=0.025$.

REFERENCES

- 1.T. Placke, R. Kloepsch, S. Duhnen, M. Winter, J. Solid State Electrochem., 21 (2017) 1939-1964.
- 2.J.M. Tarascon, M. Armand, Nature, 414 (2001) 359-367.
- 3.H. Tao, Z. Feng, H. Liu, X. Kan, P. Chen, The Open Materials Science Journal, 5 (2011) 204-214.
- 4.T. Ohzuku, A. Ueda, J. Electrochem. Soc., 142 (1995) 1431-1435.
- 5.S. Zhang, M.S. Ding, K. Xu, J. Allen, T.R. Jow, Electrochem. Solid State Lett., 4 (2001) A206-A208.
- 6.X. Sun, P. V. Radovanovic, B. Cui, New J. Chem. 39 (2015) 38-63.
- 7.T. F. Yi, S. Y. Yang, Y. Xie, J. Mater Chem. A, 3 (2015) 5750-5777.
- 8.Q. Zhang, Xi Li, Int. J. Electrochem. Sci., 8 (2013) 6449-6456
- 9 L. Li, C.Y. Liu, Y. Liu, Mater. Chem. Phys., 113 (2009) 551-557.
- 10 A.Y. Shenouda, K.R. Murali, J. Power Sources, 176 (2008) 332-339.
- 11 B. VikramBabu, K.V. Babu, G.T. Aregai, L.S. Devi, B. M. Latha, M. S. Reddi, K. Samatha, V. Veeraiah, Results in Physics, 9 (2018) 284-289.
- 12 T F. Yi, J. Shu, Y.R. Zhu, X.D. Zhu, R. S. Zhu, A.N. Zhou, J. Power Sources, 195 (2010) 285-288.
- C.M. Chang, Y. C. Chen, W.L. Ma, Y.W. C. Yang, RSC Advances, 5(61) (2015) 49248-49256
- 13 .A.Y. Shenouda, K.R. Murali, J. Power Sources, 176 (2008) 332-339.
- 14 .B. VikramBabu, K.V. Babu, G.T. Aregai, L.S. Devi, B. M. Latha, M. S. Reddi, K. Samatha, V. Veeraiah,
- 15 .Results in Physics, 9 (2018) 284-289.
- 16 .C. C. Yang, H. C. Hu, S.J. Lin, W. C. Chien, J. Power Sources, 258 (2014) 424.

- 17 .C.M. Chang, Y. C. Chen, W.L. Ma, Y.W. C. Yang, RSC Advances, 5(61) (2015) 49248-49256.
- 18 .T F. Yi, J. Shu, Y.R. Zhu, X.D. Zhu, R. S. Zhu, A.N. Zhou, J. Power Sources, 195 (2010) 285-288.
- 19.N. Rangelova, L. Aleksandrov, S. Nenkova, J. Sol-Gel Sci Technol., 85 (2018) 330-339.
- 20 .H.N. Ng, C. Calvo, Can. J. Chem., 50 (1972) 3619-3624.